International Journal of Nanoelectronics and Materials
Volume 12, No. 2, Apr 2019 [185-192]

The Effect of SrO Doping on $LaFeO_3$ using Yarosite Extraction based Ethanol Gas Sensors Performance Fabricated by Coprecipitation Method

Endi Suhendi[1*], Muhamad Taufik Ulhakim[1], Andhy Setiawan[1] and Dani Gustaman Syarif[2]

[1]*Program Studi Fisika, Universitas Pendidikan Indonesia, Bandung, Indonesia.*
[2]*Pusat Sains dan Teknologi Nuklir Terapan, Badan Tenaga Nuklir Nasional, Bandung, Indonesia.*

Received 28 September 2018, Revised 17 October 2018, Accepted 11 December 2018

ABSTRACT

Nowadays, semiconductor is one of the most important materials in the application of science and technology, especially gas sensor. In this present work, characterization of undoped and doped 10 mol% SrO on $LaFeO_3$ based ethanol gas sensors has been conducted using $LaCl_3.7H_2O$, Fe_2O_3 from yarosite extraction, and $SrCl_2.6H_2O$. The used materials were prepared through coprecipitation method. The ethanol gas sensors were made in the form of the thick film using screen printing techniques and fired at 600°C for 2 hours. Characterization of crystal and morphology structures was carried out using X-ray Diffraction (XRD) and Scanning Electron Microscopy (SEM), respectively. Electrical properties of ethanol gas sensors were examined using a gas chamber. The XRD analysis indicated that thick films had a cubic crystal structure. The SEM analysis showed that doped 10 mol% SrO decreased the grain size of $LaFeO_3$ from 31.29 nm to 29.56 nm. The analysis of electrical properties showed that the thick film doped by 10 mol% SrO has a higher response compared to undoped SrO. The operating temperature of thick films doped by 10 mol% SrO is 295°C-300°C, this value is lower than the undoped SrO operating temperature, it's 345°C – 355°C. Electrical properties indicated that thick film doped by 10 mol% SrO is the best sensor. These results show that yarosite extraction can be used as the main material in gas sensor fabrication.

Keywords: $LaFeO_3$, Yarosite, Ethanol Gas Sensor, SrO Doping, A Coprecipitation Method.

1. INTRODUCTION

The gas sensor is one of the crucial components used in daily life to detect harmful gases [1]. One type of gas sensor that is widely used and being developed is a semiconductor-based gas sensor or the so-called metal oxide semiconductor [2]. Ethanol is the most common compound that can be extensively used in a gas sensor for various applications such as biomedicine, hospital, safety, food packaging testing, and drivers' breath analyser which can help reduce the number of accidents [3]. Some types of gas sensor have been developed by Sunghoon Park [4], Chang Su [5], Lili Wang [6], Cheng Wang [7], and Zihua Wang [8].

The metal oxide semiconductor based gas sensor can be made from various materials such as Fe_2O_3 [9], SnO_2 [10], ZnO [11], and $LaFeO_3$ [12]. $LaFeO_3$ is the appropriate material for gas sensor and has a good response to ethanol gases [13-14]. Some impurities can be added to the main material in order to obtain a good response from ethanol gas sensor as successfully done by Thaweechai [15]. Thaweechai [15] used metal-organic decomposition and found that Sr doping on $LaFeO_3$ produced a good response [15]. The augmentation of the doping agent may

* Corresponding Author: *endis@upi.edu*

cause the grain size shrinkage of the material used. According to Zhang (2015), if the grain size is smaller, the response will be better [16].

In this paper, the researchers have synthesized $LaFeO_3$ and $LaFeO_3$ doped by 10 mol% of SrO using coprecipitation method for ethanol gas sensor. The researchers chose to add the 10 mol% of SrO as a dopant based on the result from Thaweechai research which found that the sensor will have a lower response if the dopant is more than 10 mol%. Therefore, the 10 mol% was the proper amount of dopant for improving the ethanol sensing properties on $LaFeO_3$-based sensor [15]. One of the materials that the researchers used in this study were yarosite extraction. The use of yarosite extraction is to investigate and prove that natural materials have good characteristics that are applicable in gas sensors. The coprecipitation method was employed in this study because this method is able to produce smaller grain size or even the nanoparticles [17].

2. MATERIALS AND METHODS

2.1 Preparation of Undoped and Doped 10 mol% on $LaFeO_3$ Powders

The materials were synthesized by coprecipitation method of $LaCl_3.7H_2O$, Fe_2O_3 from yarosite extraction, and $SrCl_2.6H_2O$. In this study, two material were made: the undoped, and the doped 10 mol% SrO on $LaFeO_3$. The first material is undoped $LaFeO_3$. The material was prepared by mixing the solution of $LaCl_3,7H_2O$, and the solution of Fe_2O_3 from yarosite extraction. The second material is doped with 10 mol% of SrO on $LaFeO_3$. The material was prepared by mixing the solution of $LaCl_3.7H_2O$, the solution of Fe_2O_3 from yarosite extraction and the solution of $SrCl_2.6H_2O$. To prepare both solutions, each material is dissolved in aquadest. To make the solution of Fe_2O_3, the material was dissolved in acid. Then, ammonia hydroxide (NH_4OH 25%) were added to each mixed solutions to produce the precipitate of undoped and doped 10 mol% SrO on $LaFeO_3$. Both precipitates were dried at 100°C for 6 hours and then calcined at 600°C for 2 hours and 800°C for 3 hours. After that, both materials were respectively crushed into powders.

2.2 Thick Film Fabrication

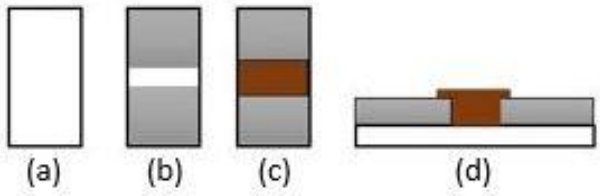

Figure 1. (a) Alumina substrate (b) Alumina substrate coated with silver (c) Alumina substrate which has been coated in silver and coated again with the material paste, and (d) The thick films viewed from the side.

Thick films of undoped $LaFeO_3$ and doped 10 mol% SrO on $LaFeO_3$ were fabricated using screen printing techniques. Firstly, the alumina substrate was coated with silver and burned at 600°C for 10 minutes. Then, the silver-coated substrate was coated with a paste of materials and burned at 600°C for 2 hours. The illustration of the thick film is shown in Figure 1. The paste materials are a mixture of the main material powders and an organic vehicle. In this study, the mixture consist of 70% main material and 30% organic vehicle.

2.3 Characterization of Thick Films

2.3.1 Structural and Morphology Characterization

Structural characterizations were carried out using X-ray Diffraction (XRD) and Scanning Electron Microscopy (SEM). XRD characterization was done by firing x-ray with Cu $K_\alpha 1$ wavelength ($1{,}5406\ x\ 10^{-10}$m) using PANanalytical X'Pert Pro Series PW3040/x0 X'Pert Pro. From this analysis, the average of crystallites sized and the lattice parameters were found. The average of crystallites sized was calculated using Debye-Scherrer as shown in equation Equation (1) [18].

$$D = \frac{0.89\lambda}{B\cos\theta} \quad (1)$$

where λ is the wavelength of x-ray source and B is the full at half-maximum intensity (FWHM) in radians of a peak at Bragg's angle θ.

SEM characterization was done by Analysis Scanning Electron Microscopy JEOL JSM – 6360LA. From this analysis, the grain size was found by comparing the image scale produced with the benchmark scale of the magnification performed.

2.3.2 Electrical Properties

The characterization of electrical properties was conducted to recognize the electrical properties of the thick film of undoped and doped 10 mol% of SrO which applied as ethanol gas sensor. This characterization was performed by measuring the resistance at each 5°C temperature change under ambient condition (without ethanol) and in the condition that contains ethanol gas. The resistance was measured using a multimeter connected to a probe in the gas chamber as shown in Figure 2 below.

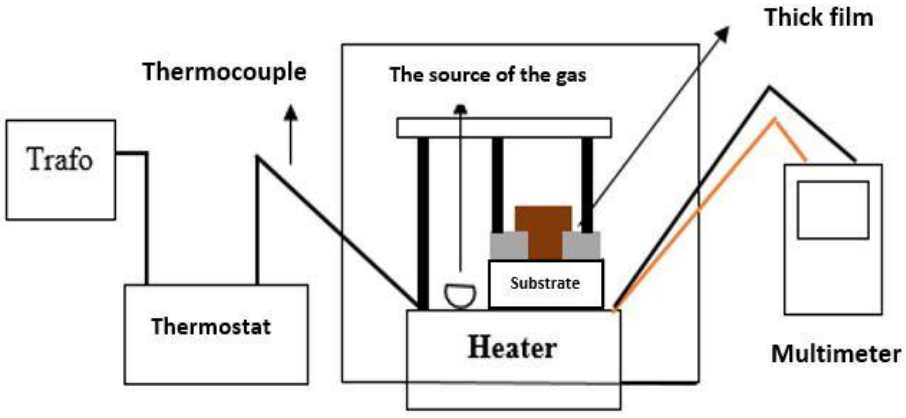

Figure 2. Design of resistance measurement devices.

The results of this characterization were response and operation temperature. That result was obtained from the calculation by using the Equation (2) [19-25].

$$\text{Response} = \frac{\Delta R}{R_a} = \frac{R_g - R_a}{R_a} \quad (2)$$

where R_g is the resistance of the gas sensor in a test containing ethanol, and R_a is the air resistance of the gas sensor.

3. RESULTS AND DISCUSSION

3.1 Crystal Structure and Morphology Characterizations

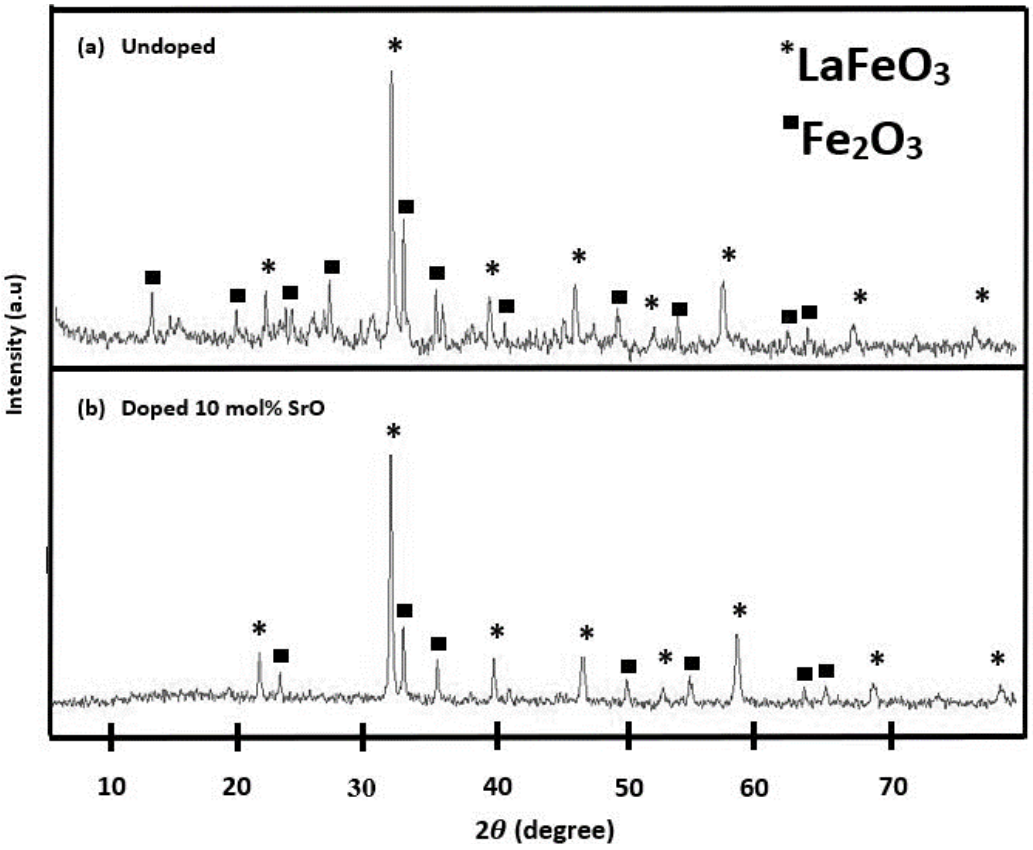

Figure 3. XRD pattern of undoped $LaFeO_3$ and doped 10 mol% SrO on $LaFeO_3$ on thick films.

The XRD patterns of undoped $LaFeO_3$ and doped 10 mol% SrO on $LaFeO_3$ are shown in Figure 3. The patterns show that both materials had two phases i.e $LaFeO_3$ as the main phase and Fe_2O_3 as the second phase. XRD analysis shows that both materials had cubic structure which indicated with (100), (101), (111), (200), (201), (211), (202), and (301) planes, those diffraction data are referring to JCPDS card of $LaFeO_3$ (JCPDS No. 96-154-2033).

The average of crystallite size has been calculated using Debye-Scherrer's formula as shown in Equation (1). It was found that the crystallite size decreased when 10 mol% of SrO is added to the main material.

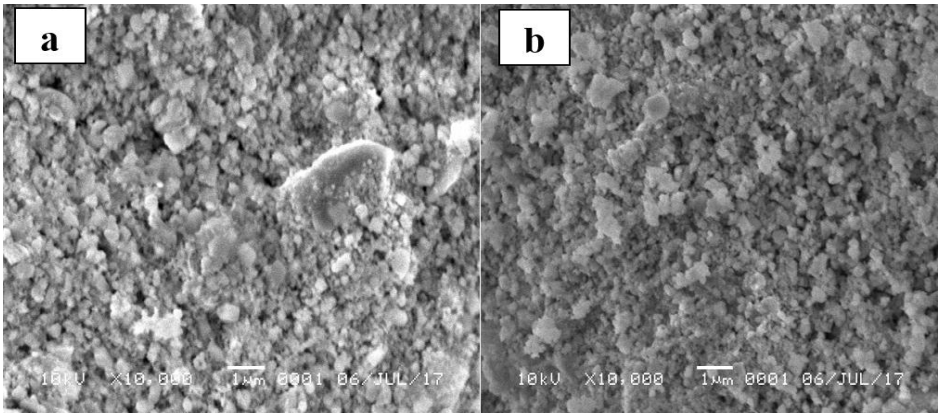

Figure 4. SEM characterization images of (a) undoped and (b) doped 10 mol% SrO on $LaFeO_3$.

This study also investigated the average grain size using the Scanning Electron Microscopy (SEM) as shown in Figure 4. SEM images of undoped $LaFeO_3$ and doped 10 mol% SrO on $LaFeO_3$ were taken in the form of thick films which calcined at 600°C for 2 hours and 800°C for 3 hours. In this investigation, it was found that the size of grain decreased when dopant was added to the main material.

Crystallites size and grain size decreased when 10 mol% of SrO was added on $LaFeO_3$. Its caused Sr^{2+} ion to successfully substituted La^{3+} ion on $LaFeO_3$. It worked because the size of the radius ionic of La^{3+} (0.13nm) does not have a significant difference with the size of the radius ionic of Sr^{2+} (0.14 nm) [26-27]. The results were summarized in Table 1below.

Table 1 Structure and morphology characterization results of undoped $LaFeO_3$ and doped 10 mol% SrO on $LaFeO_3$

Compounds	Undoped	Doped 10 mol% SrO
Lattice parameters a = b = c = Å	3.8977	3.9516
Crystallites size D (nm)	31.29	29.56
Grain size (μm)	0.42	0.26

3.2 Electrical Properties Characterization

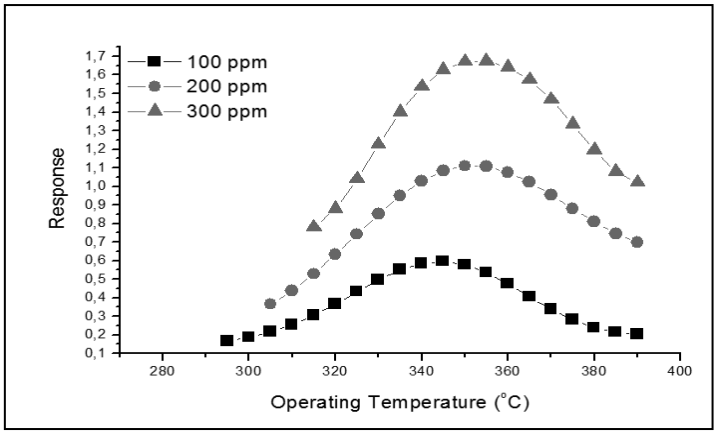

(a)

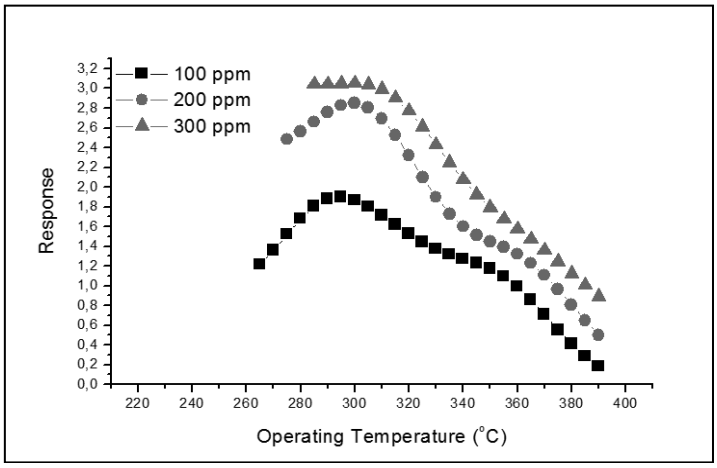

(b)

Figure 5. Response to ethanol of (a) undoped and (b) doped 10 mol% SrO on $LaFeO_3$ on gas concentration variation.

Response and operating temperature are two components that influence metal oxide semiconductor gas sensing. In this study, the relationship between response and operating temperature was investigated in various gas concentration as shown in Figure 5. The response was calculated by using the formula shown in Equation (2).

Figure 5 suggests that the response of gas sensor based undoped and doped 10 mol% SrO on $LaFeO_3$ increases with the increase of ethanol gas concentration. However, a higher response was shown by the doped 10 mol% SrO on $LaFeO_3$ based gas sensor. The results were summarized in Table 2.

Table 2 Sensing performance of gas sensor based undoped $LaFeO_3$ and doped 10 mol% SrO on $LaFeO_3$

Compounds	Gas concentration (ppm)	Response	Operating temperature (°C)
Undoped	100	0.60	345
	200	1.11	350
	300	1.67	355
Doped by 10 mol% of SrO	100	1.90	295
	200	2.86	300
	300	3.05	300

In this study, gas sensing performance shows that undoped $LaFeO_3$ and doped 10 mol% SrO on $LaFeO_3$ were p-type metal oxide semiconductor gas sensor. According to Murade (2010), the type of metal oxide semiconductor can be recognized from electrical properties characterization. If the resistance of the gas sensor exposed to ethanol is greater than the ambient, then the gas sensor belongs to p-type. If the resistance of the gas sensor, when added by ethanol, is smaller than the ambient, the gas sensor belongs to n-type [26].

The sensing mechanism of p-type metal oxide semiconductor gas sensor is the absorption of oxygen gas molecules on the oxide surface in the form of oxygen ions as shown by the chemical reaction in Equation (3) [28-29]. When the oxygen molecules were absorbed, the number of electrons on the oxide surface will decrease and the number of holes produced will increase [25].

$$\frac{1}{2}(O_2)_{gas} \rightarrow (O^-)_{adsorption} + h^+(lattice) \quad (3)$$

As the ethanol gas was introduced to sensor gas based undoped $LaFeO_3$ and doped 10 mol% of SrO on $LaFeO_3$, the chemical reaction may occur as shown in Equation (4) [30-31]. Based on Equation (4), the oxygen in the air will be absorbed by the gas sensor surface and captured the electrons of the gas sensor, hence, increasing holes and recovery of the resistance to the initial state [32].

$$C_2H_5OH_{gas} + 6O^{n-}{}_{(ads)} \rightarrow 2CO_2ads + 3H_2O_{ads} + 6ne \quad (4)$$

4. CONCLUSION

In this study, the materials of undoped $LaFeO_3$ and doped with 10 mol% of SrO on $LaFeO_3$ powders have been synthesized by co-precipitation method for ethanol gas sensor application. XRD characterization indicates that the materials had a cubic structure with the crystallites size of 31.29nm and 29.56nm, respectively. The materials contain two phases i.e $LaFeO_3$ and Fe_2O_3. SEM characterization showed that doped 10 mol% SrO decreased the grain size of $LaFeO_3$. The analysis of the electrical properties showed that the response of thick film based gas sensor to ethanol gas increased with ethanol gas concentration. The thick film based $LaFeO_3$ doped 10

mol% SrO have a better response. It was found that the operating temperature for ethanol gas sensor based undoped and doped 10 mol% SrO were 345℃-355℃ and 295℃-300℃, respectively.

ACKNOWLEDGEMENT

This work was financially supported by "Hibah Penelitian Terapan Unggulan Perguruan Tinggi" Research Grants in the fiscal year 2018.

REFERENCES

[1] Xiao, H., Xue, C., Song, P., Li, J., Wang, Q, Applied Surface Science. **337** (2015) 65-71.
[2] Jin, C., Ge, C., Xu, G., Peterson, G., Jian, Z., Wei, Y., Zhu, K., Materials Science and Engineering B. **224** (2017) 158-162.
[3] Shaikh, F. I., Chikhale, L. P., Mulla I. S., Suryavanshi, S. S., J Mater Sci: Mater Electron. **28** (2017) 3128-3139.
[4] Park, S., Kim, S., Sun G.J., Lee, C., ACS Appl. Mater. Interfaces. **7**, 15 (2015) 8138-8146.
[5] Su, C., Li, Y., He, Y., Liu, L., Wang, X., Liu, L., Materials Science in Semiconductor Processing. **39** (2015) 49-53.
[6] Wang, L., Lou, Z., Deng, J., Zhang, R., Zhang, T., ACS Appl. Mater. Interfaces **7**, 23 (2015) 13098-13104.
[7] Wang, C., Cui, X., Liu, J., Zhou, X., Cheng, X., Sun, P., Hu, X., Li, X., Zheng, J., Lu, G., ACS Sens. **1**, 2 (2015) 131-136.
[8] Wang, Z., Tian, Z., Han D., Gu, F., 2016. ACS Appl. Mater. Interfaces. **8**, 8 (2016) 5466-5474.
[9] Guo, X., Zhang, J., Ni, M., Liu, L., Lian, H., Wang, H., J Mater Sci: Mater Electron. **27** (2016) 11262-11267.
[10] Wang, Y., Liu, C., Wang, L., Liu, J., Zhang, B., Gao, Y., Sun, P., Sun, Y., Zhang, T., Lu, G., Sensor and Actuator B: Chemical. 240 (2016) 1321-1329.
[11] Ruchika, V. K. Anand, S. C. Sood & G. S. Virdi, "Fabrication and characterization of zinc oxide based thick and thin film ethanol sensors doped with aluminium oxide," Int. Journal of Applied Sciences and Engineering Research, **5** (2016) 81-89.
[12] Benali, A., Azizi, S., Bejar, M., Dhahri, E., Graca, M. F. P., Ceramics International. **40** (2014) 14367-14373.
[13] Fan, H., Zhang, T., Xu, X., Lv, N., Sensors and Actuator B: Chemical. **153** (2010) 83-88.
[14] Khetre, S. M., Jadhav, H. V., Jagadale, P. N., Kulal, S. R., Bamane, S. R., Adv. Appl. Sci. Res. 2, 4 (2011) 503-511.
[15] Thaweechai, T., Wisitsoraat, A., Laobuthee, A., Koonsaeng, N., Kasetsart J. (Nat. Sci.). **43** (2009) 218-223.
[16] Zhang, X., Gu, R., Zhao, J., Jin, G., Zhao, M., Xue, Y., Journal of Materials Engineering and Performance. 24 (2015) 3815-3819.
[17] Irfan, S., Ajaz-un-Nabi, M., Jamil, Y., Amin, N., "IOP. Conf. Ser.: Mater. Sci, Eng. 60 (2014) 1-5.
[18] Li, Z., Yi, J., Sensor and Actuator B: Chemical. 234 (2016) 96-103.
[19] Olejnik, R., Slobodian, P., Riha, P., Saha, P., Journal of Materials Science Research. **1** (2012) 105-106.
[20] Kamble, V., Umarji, A.M., Electronic Supplementary Material (ESI) for Journal of Materials Chemistry, (2013).
[21] Tian, W. C., Ho, Y. H., Chen, C. H., Kuo, C. Y., Sensors (Basel). **13**, 1 (2013) 865-874.
[22] Zhan, S., Li, D., Liang, S., Chen, X., Li, X., Sensors (Basel). **13**, 4 (2013) 4378-4389.
[23] Kapse, V. D., Raghuwanshi, F. C., Sangawar, V. S., International Journal of Chemical and Physical Sciences (IJCPS). **4** (2015) 121-127.

[24] Cho, S. Y., Yoo, H. W., Kim, J. Y., Jung, W. B., Jin, M. L., Kim, J. S., Jeon, H. J., Jung, H. T., Nano Lett. 16, 7 (2016) 4508-4515.
[25] Suhendi, E., Witra, Hasanah, L., Syarif, D. G., AIP Conf. Proc. **1848** (2017) 050008.1-050008.4.
[26] Murade, P. A., Sangawar, V. S., Chaudhari, G. N., Kapse, V. D., Bajpeyee, A. U., Current Applied Physics. **11** (2010) 451-456.
[27] Cyza, A., Kopia, A., Cieniek, L., Kusinski, J., Material Today: Proceedings, 6th International Conference on Advanced Nano Materials. **3** (2016) 2707-2712.
[28] Choi, Y. H., Kim, D. H., Hong, S. H., Hong, K. S., Chemical. **178** (2013) 395-403.
[29] Choi, Y. H., Kim, D. H., Hong, S. H., Sensor and Actuator B: Chemical. **243** (2016) 262-270.
[30] Doroftei, C., Popa, P. D., Lacomi, F., Sensor and Actuator A: Physical. **190** (2012) 176-180.
[31] Doroftei, C., Popa, P.D., Lacomi, F., Leontie, L., Sensor and Actuator B: Chemical. **191** (2013) 239-245.
[32] Cao. E., Yang, Y., Cui, T., Zhang, Y., Hao, W., Sun, L., Peng, H., Deng, X., Applied Surface Science. **393** (2016) 134-143.